

# High-Resolution Structure of Murine Interleukin 1 Homologue IL-1F5 Reveals Unique Loop Conformations for Receptor Binding Specificity<sup>†,‡</sup>

Eleanor F. Dunn,<sup>§</sup> Nicholas J. Gay,<sup>⊥</sup> Adrian F. Bristow,<sup>||</sup> David P. Gearing,<sup>#</sup> Luke A. J. O'Neill,<sup>§</sup> and Xue Yuan Pei<sup>\*,§,⊥</sup>

Department of Biochemistry, Trinity College, Dublin 2, Ireland, Department of Biochemistry, University of Cambridge, Tennis Court Road, Cambridge CB2 1GA, UK, National Institute for Biological Standards and Controls, South Mimms, Potters Bar, Herts, EN6 3QG, UK, and CSL Limited, 45 Poplar Road, Parkville, VIC 3052, Australia

Received January 21, 2003; Revised Manuscript Received June 20, 2003

**ABSTRACT:** Interleukin-1 (IL-1) F5 is a novel member of the IL-1 family. The IL-1 family are involved in innate immune responses to infection and injury. These cytokines bind to specific receptors and cause activation of NF $\kappa$ B and MAP kinase. IL-1F5 has a sequence identity of 44% to IL-1 receptor antagonist (IL-1Ra), a natural antagonist of the IL-1 system. Here we report the crystal structure of IL-1F5 to a resolution of 1.6 Å. It has the same  $\beta$ -trefoil fold as other IL-1 family members, and the hydrophobic core is well conserved. However, there are substantial differences in the loop conformations, structures that confer binding specificity for the cognate receptor to IL-1 $\beta$  and the antagonist IL-1Ra. Docking and superimposition of the IL-1F5 structure suggest that it is unlikely to bind to the interleukin1 receptor, consistent with biochemical studies. The structure IL-1F5 lacks features that confer antagonist properties on IL-1Ra, and we predict that like IL-1 $\beta$  it will act as an agonist. These studies give insights into how distinct receptor specificities can evolve within related cytokine families.

Interleukin-1 F5 (IL-1F5),<sup>1</sup> a novel member of the IL-1 family, shows significant sequence identity to the interleukin 1 receptor antagonist (IL-1Ra). The classical members of the IL-1 family (IL-1 $\alpha$ , IL-1 $\beta$ , IL-1Ra, and IL-18) are cytokine ligands all involved in controlling inflammatory and immune responses (1). IL-1 $\alpha$ , IL-1 $\beta$ , and IL-18 are agonists in these responses. They bind their cognate receptors, IL-1RI and IL-18R, as binary complexes and recruit accessory proteins (IL-1RAcP and IL-18RAcP) to form the active signaling complex (2). The signaling pathways initiated by them lead to activation of MAP kinases and the transcription factor NF $\kappa$ B (3). By contrast, IL-1Ra inhibits the actions of IL-1 at IL-1RI, binding to the receptor but not activating any signaling pathways (4). More recently, six new members of the IL-1 family have been discovered, named IL-1F5 to IL-1F10 (5). Sequence identity over the family ranges from 13 to 56%, and particular interest has been focused on the similarity between IL-1F5 and IL-1Ra. Although no IL-1Ra like activity has been found for IL-1F5 (6), activation of an NF $\kappa$ B reporter system by IL-1F9 is inhibited by IL1F5 in cells transfected with IL-1Rrp2 (7). The extracellular regions

of IL-1RI and IL-18R consist of three immunoglobulin-like domains (Ig domains) and belong to a family with a further six members including IL-1RII, T1/ST2, IL-1Rrp2, APL, TIGGIR, and SIGGIR (2).

The crystal structures of both IL-1 $\beta$  and IL-1Ra have been solved as free ligands (8–11) and in complex with IL-1RI (12, 13). The two structures have the same overall  $\beta$ -trefoil fold but differ somewhat in loop length and structure. IL-1Ra binds to IL-1RI predominantly through interaction with domains 1 and 2 of the receptor, whereas IL-1 $\beta$  makes additional contacts with the membrane proximal domain 3, resulting in a rotation of this domain by about 20° relative to that of the IL-1Ra bound receptor. It is the interaction of IL-1 $\beta$  with domain 3 that is thought to bring about the conformation required to recruit the IL-1RAcP and activate signaling. The structure of a trimeric complex of IL-1/IL-1RI/IL-1RAcP has not been determined, but site-directed mutagenesis experiments imply that certain amino acid residues that do not affect receptor binding nevertheless impair biological activity, probably due to their involvement in the IL-1RAcP interaction. In particular, Lys145 of IL-1Ra when converted to Asp, as found in IL-1 $\beta$ , converts the antagonist to a partial agonist (14). This residue may therefore be critical for the recruitment of the accessory protein and for signal transduction.

Here we present the structure of murine IL-1F5 determined by molecular replacement at 1.6 Å resolution. We examine its structure in comparison to both IL-1 $\beta$  and IL-1Ra, and identify regions of unique conformation. In conjunction with the ligand bound IL-1RI structure and IL-1 mutagenesis studies, we found that there are potential sites of receptor

<sup>†</sup> This work was funded by the EU Fifth Framework, Grant Number QLGI CT 1999 00549 (PATOLLOGY) awarded to N.J.G. and L.O.'N.

<sup>‡</sup> PDB code of IL-1F5: 1MD6.

\* To whom correspondence should be addressed: Xue Y. Pei and Luke A. J. O'Neill; e-mail: xyp20@mole.bio.cam.ac.uk and laoneill@tcd.ie.

<sup>§</sup> Trinity College.

<sup>⊥</sup> University of Cambridge.

<sup>||</sup> National Institute for Biological Standards and Controls.

<sup>#</sup> CSL Limited.

<sup>1</sup> Abbreviations: IL-1, interleukin 1; IL-1RI, type 1 interleukin 1 receptor.

Table 1: Lattice and Refinement Statistics: X-ray Structure Determination

data collection and processing		refinement statistics	
space group	<i>P</i> 3221	resolution (Å)	39.5–1.6
cell dimension (Å)	78.9, 78.9, 69.7, 90, 90, 120	<i>R</i> factor (%)	20.2
resolution (Å)	39.5–1.58	<i>R</i> free factor (%)	21.2
wavelength (Å)	0.934	weighted rmsd from ideality	
no of unique reflections	40560	bond length (Å)	0.005
mean redundancy (outer shell)	6.5 (7.0)	bond angle (degree)	1.4
overall <i>R</i> <sub>sym</sub> (outer shell) (%)	7.8 (47.8)	dihedral angle (degree)	24.7
<i>I</i> / <i>σ</i> ( <i>I</i> ) (outer shell)	4.7 (1.4)	total no. of protein atoms	1185
<i>B</i> overall (by Patterson) (Å <sup>2</sup> )	24.4 24	no. of waters	182
		mean <i>B</i> value, protein (Å <sup>2</sup> ) (main chain/side chain)	19.8/23.1
		mean <i>B</i> value, water (Å <sup>2</sup> )	37

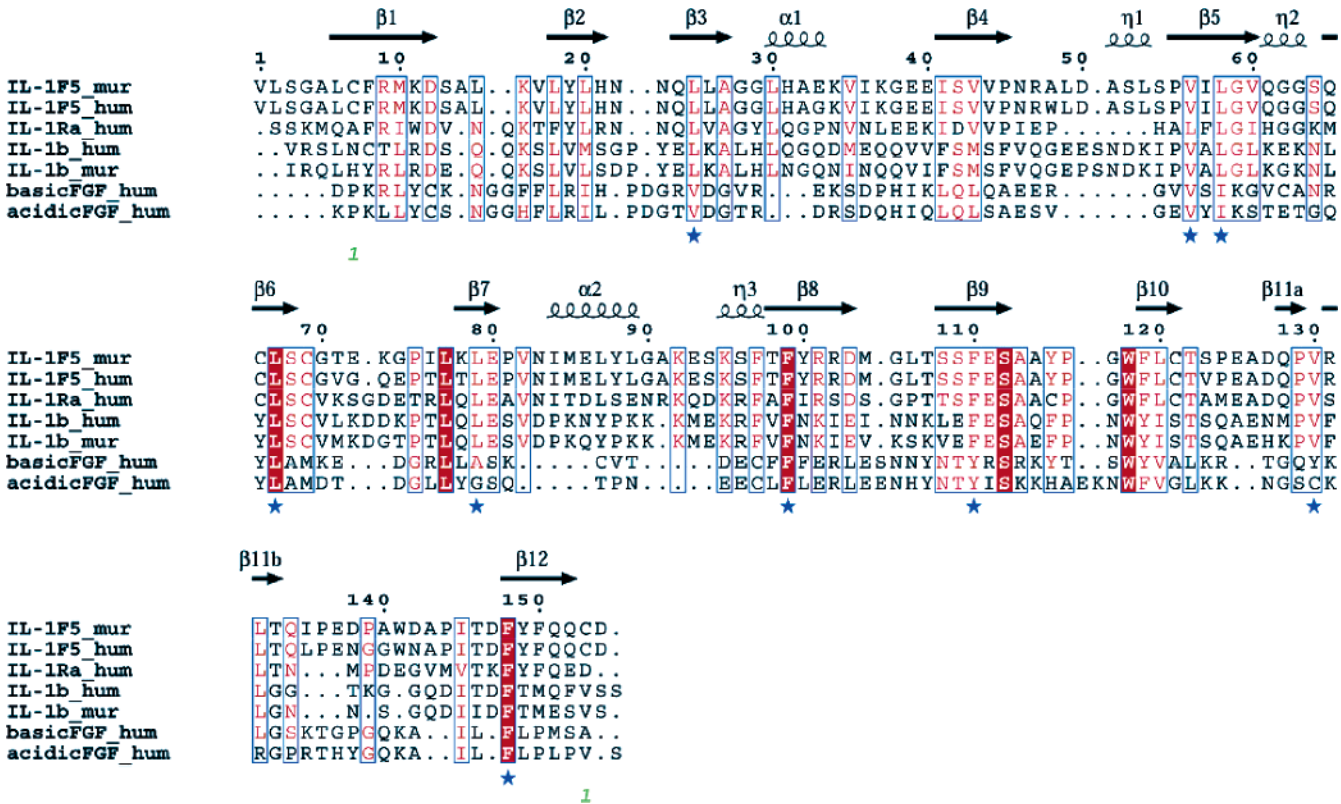


FIGURE 1: Structure-based sequence alignment of IL-1 homologues. Sequences were collected using a psi-Blast search were aligned using CLUSTALW and FUGUE (27, 28). The alignment consists of murine IL-1F5 with six other members of the  $\beta$ -trefoil family; IL-1Ra<sub>hum</sub>, human IL-1Ra (1IRP); IL-1 $\beta$ <sub>hum</sub>, human IL-1 $\beta$  (111B); IL-1 $\beta$ <sub>mur</sub>, murine IL-1 (2MIB); basicFGF<sub>hum</sub>, human basic fibroblast growth factor (2FGF); acidicFGF<sub>hum</sub>, human acidic fibroblast growth factor (2AFG); the sequence of human IL-1F5 (IL-1F5<sub>hum</sub>) is also included.  $\beta$ -strands and helical structures of IL-1F5 are indicated with arrows and coils, respectively, and numbered according to their succession. The cysteines that form a disulfide bond in IL-1F5 are also indicated by the green digit 1, and conserved residues which contribute to the hydrophobic core are highlighted with a blue star. Residues are colored according to percentage equivalence.

binding and accessory protein interaction in the IL-1F5 structure.

EXPERIMENTAL PROCEDURES

*Expression and Purification of IL-1F5.* The gene encoding the murine IL-1F5 was inserted into pET21a expression vector using NdeI and EcoRI restriction sites. The resulting plasmid was transformed into *Escherichia coli* cell line BL21(DE3). A single colony was used to inoculate 100 mL of M9 medium supplemented with 5 g/L yeast extract and 100  $\mu$ g/mL ampicillin and was grown overnight at 37  $^{\circ}$ C. This overnight culture was diluted 1 in 40 with the supplemented M9 medium and grown to an OD<sub>600</sub> of 0.6 at 37  $^{\circ}$ C. The culture was then induced with IPTG for 3 h at a final concentration of 1 mM. Cells were harvested by centrifugation and frozen at  $-80^{\circ}$  C overnight. Pellets were

then thawed and resuspended in 150 mL of NETN buffer (20 mM Tris-HCl, 100 mM NaCl, 1 mM EDTA, pH 8 plus 0.5% v/v NP-40). Cell lysis was achieved by incubation at room temperature for 10 min with 200  $\mu$ g/mL lysozyme with continuous rolling, followed by sonication for 5 min with 5 s pulses followed by 5 s of cooling. The suspension was then cleared of insoluble material by centrifugation (38000g) for 1 h. The soluble fraction was then precipitated with 50% ammonium sulfate and pelleted by centrifugation at 12 000 rpm for 2 h. The supernatant was discarded, and the pellet was stored at 4  $^{\circ}$ C until use. The precipitated protein was resuspended in 8 mL/L culture of 50 mM ammonium acetate and applied to a preequilibrated sephadex G75 column (Pharmacia). Fractions were collected and analyzed by SDS-PAGE, and those containing IL-1F5 were pooled for further chromatography. Fractions were freeze-dried and resus-

pended in 1 mL/L culture of 25 mM Tris-HCl, pH 8 and loaded on a MonoQ column (Pharmacia) and eluted with an increasing salt gradient of NaCl from 0 to 1 M NaCl. Two milliliter fractions were collected, and IL-1F5 was found to elute from the column at a concentration of 100 mM NaCl. Protein was dialyzed into water before use in crystallization. N-terminal amino acid sequencing and mass spectrometric analysis confirmed the identity of the purified protein as murine IL-1F5.

**Protein Crystallization.** Crystallization screens were carried out using the vapor diffusion method in a hanging drop. Crystal screen and crystal screen 2 from Hampton Research were used. Protein at 5 mg/mL was mixed with precipitant at a volume ratio of 1:1, and the drop is placed over the reservoir of the precipitant at 18 °C. Crystals appeared at 18 °C in two conditions, 10 mM cobalt chloride, 0.1 M KCl, 0.1 M HEPES, pH 7.5, 1.5 M ammonium sulfate, and 0.1 M KCl, 0.1 M HEPES, pH 7.5, 1.5 M ammonium sulfate, respectively. Single crystals were obtained in 0.1 M KCl, 0.1 M HEPES, pH 7.5, 1.3 M ammonium sulfate by micro seeding. A typical crystal grew to a size of  $0.2 \times 0.08 \times 0.1$  mm at 18 °C in 10–14 days. Crystals were flash frozen in liquid nitrogen stream at 100 K in cryoprotectant containing the precipitant and 25% glycerol. IL-1F5 crystallizes in space group of  $P3_221$  with unit cell dimensions of  $a = 78.93$  Å,  $c = 69.74$  Å. There is one molecule in an asymmetric unit with corresponding solvent content of 62.2% and Matthews' coefficient of 3.28 (see Table 1).

**X-ray Data Collection and Processing.** X-ray diffraction data of single IL-1F5 crystal was collected at a resolution of 1.5 Å at beam line ID14 EH2, Grenoble, France. Data were processed at a resolution of 1.58 Å with MOSFLM (15). Data were sorted, scaled, and truncated using CCP4 package (16) (Table 1). For further details of phase determination and refinement, see Supporting Information.

**Homology Modeling and Docking.** Homologues of IL-1F5 were searched using BLAST against a nonredundant database. Sequence alignment of homologues was performed using ClustalW (17) and subsequently edited by hand. The alignment was used to generate a 3D model of murine IL-1Rrp2 extracellular region (GB, gi 10644684) and was computed with MODELLER (18) using the structure of human IL-1RI (1ITB) as a template. The model with the lowest energy and best geometry was selected and checked with PROCHECK (19). IL-1F5 was docked to IL-1RI using GRAMM 400 (20).

## RESULTS AND DISCUSSION

**High-Resolution Crystal Structure of IL-1F5.** IL-1F5 has 44 and 24.5% sequence identity to human IL-1Ra and IL-1 $\beta$ , respectively; therefore, it is expected that, like IL-1Ra and IL-1 $\beta$ , it folds into a  $\beta$ -trefoil structure (Figure 2). This places it in a structural family that includes fibroblast growth factor (FGF) (21), histactophilin (22), and soyabean trypsin inhibitor (23). Figure 1 gives an alignment of seven family members with the structure elements we find in IL-1F5 indicated. IL-1F5 consists of 12  $\beta$ -strands and 11 connecting loops named according to the strands they connect (Figure 2). Val130 disrupts strand 11, and by comparison with IL-1 $\beta$  these are designated 11a and 11b. Strands 1, 4, 5, 8, 9, and 12 fold to make a six-stranded antiparallel  $\beta$ -barrel,

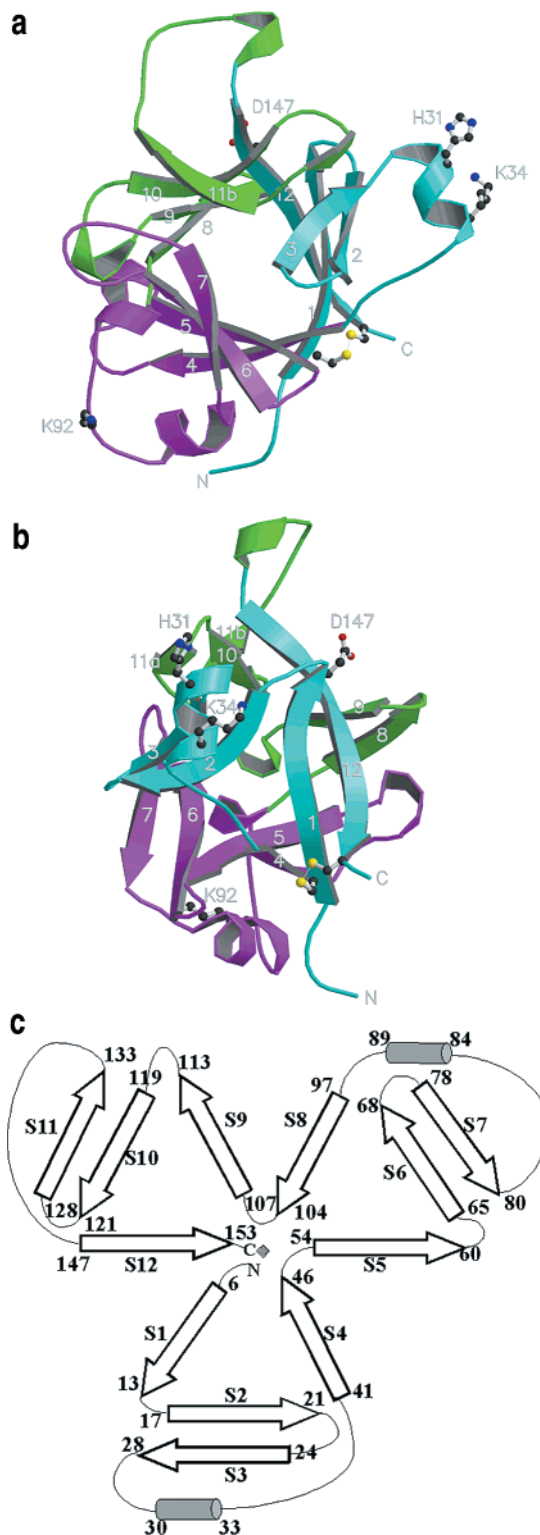


FIGURE 2: Crystal structure of IL-1F5. Ribbon diagrams were generated using MOLSCRIPT and RASTER3D (29) orientated down (a) and perpendicular (b) to the barrel axis. Highlighted by ball-and-stick representation are the cysteines involved in the disulfide (which is indicated with a thin line) and residues from loop 3–4; His31 and Lys34, loop 7–8; Lys92, postulated to be in the receptor interaction region and Asp147 postulated to interact with accessory protein. Nitrogen, oxygen, carbon and sulfur are colored blue, red, black and yellow, respectively. The  $\beta$ -strands are labeled 1 to 12. (c) Topology of the IL-1F5  $\beta$ -trefoil fold. Secondary structure elements are determined using DSSP (29).  $\beta$ -strands are indicated by arrows and helical structures by cylinders, and numbers indicate the residues at which secondary structures begin and end. Adapted and modified from Vigers et al. (12).



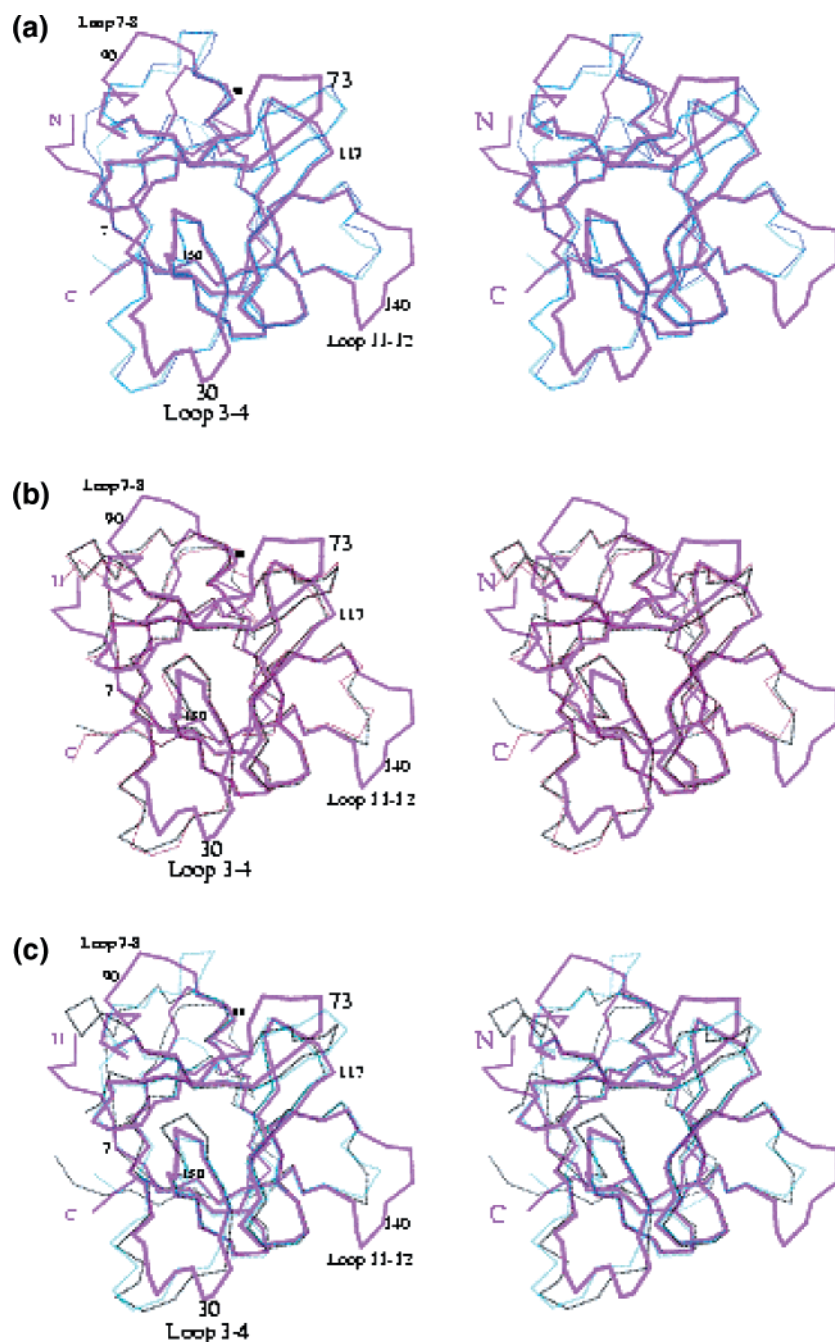


FIGURE 3: Comparison of the structure of IL-1F5 with IL-1 $\beta$  and IL-1Ra. Stereoviews of C $\alpha$ -trace of IL-1F5 (magenta) superimposed on (a) IL-1Ra: free form (cyan), bound to IL1RI (blue); (b) IL-1 $\beta$ : free form (black), bound to IL-1RI (brown); (c) free form of IL-1Ra (cyan) and IL-1 $\beta$  (black). Figures should be viewed with stereo glasses and were generated using MOLSCRIPT. Some residues and loops of IL-1-F5 are indicated.

which is closed off at one end by a cap consisting of a triangular arrangement of three  $\beta$ -hairpins. The fold as a whole may be described as consisting of three repeating units of four  $\beta$ -strands, which gives the molecule a pseudo 3-fold axis (Figure 2c). The barrel is closed off by the interaction of strands 1 and 12, which is strengthened by a disulfide bond between Cys7 and Cys153. The presence of this disulfide was confirmed using mass spectrometric analysis of alkylated fragments from IL-1F5 (data not shown). IL-1F5 therefore differs from IL-1 $\beta$ , which does not have a disulfide bridge and IL-1Ra, which does have one but in a different location, between Cys 69 and Cys116 (11).

The barrel and cap structures are packed by highly conserved hydrophobic residues, and are arranged in a

manner similar to that described for other members of the  $\beta$ -trefoil family, with layers of residues formed by alternate residues from each of the  $\beta$ -strands in the  $\beta$ -barrel and the cap packed by one residue from each strand (24).

*The Conformation of the Loops in IL-1F5 Are Substantially Different to Those of IL-1 $\beta$ .* Although the structural framework of IL-1F5 is highly conserved, the loops connecting the  $\beta$ -strands vary considerably in length and structure when compared to both IL-1 $\beta$  and IL-1Ra. Within each repeating unit the loops connecting strands 1 to 2 and 2 to 3 are hairpins belonging to a previously recognized class (25). By contrast, longer and more variable loops connect strands 3 to 4 in each repeat (see Figure 2c). The three repeating units are themselves connected by  $\beta$ -hairpins, giving a total of 11

loops. There are two helical structures that are not found in IL-1 $\beta$  or IL-1Ra: helix 1 consists of residues Leu30 to Lys34 in loop 3–4, and helix 2 is at the end of loop 7–8 from residues Ile84 to Leu89. Our analysis suggests that these are native conformations and are unlikely to be induced by crystal packing because they are stabilized by bound water molecules (see Supporting Information). In IL-1 $\beta$  these loops make specific contacts with all three domains of the IL-1R. It seems likely that the corresponding structures of IL-1F5 will also mediate specific binding to receptor.

**Comparison of IL-1F5 with IL-1 $\beta$  and IL-1Ra.** As expected from the discussion above, the overall structure of IL-1F5 is similar to IL-1 $\beta$  and IL-1Ra. The main chain C $\alpha$  atoms can be superimposed on those of IL-1 $\beta$  and IL-1Ra with RMSD values of 1.02 and 1.04 Å, respectively, including the loops. However, these values are 0.78 and 0.79 Å for the framework region alone showing that most of the structural variability is in the loops. Five major regions of divergence occur from the structure of IL-1 $\beta$  (see the stereo diagrams, Figure 3a–c).

(i) the N-terminal regions are displaced by as much as 7.5 Å from each other before the beginning of the first  $\beta$  strand.

(ii) In loop 3–4 IL-1F5 has about 1.5 turns of  $\alpha$ -helix compared to a short and differently positioned  $3_{10}$  helix in IL-1 $\beta$ . In the complexes of IL-1 $\beta$  and IL-1Ra with receptor, this  $3_{10}$  helix makes important “site A” contacts with the linker region between domains 1 and 2 of the receptor (12, 13). In IL-1F5, the side chains of His31, Lys37, and Lys39 are exposed to solvent and would be available to make corresponding interactions with the cognate receptor.

(iii) Loop 6–7 is shorter by one residue in the hairpin of IL-1F5 causing the tips of the loops to diverge such that they are 6 Å apart, with that of IL-1F5 pointing down toward the  $\beta$ -barrel.

(iv) Loop 7–8, the longest loop in IL-1F5, varies considerably from that of IL-1 $\beta$ ; helix 2, which is not found in IL-1 $\beta$  is located in this region. There is a hydrophobic patch, similar to one found in IL-1Ra and consisting of residues Val82, Leu87, and Phe97, and also contributed to by Val44 and Ile51, that is not present in IL-1 $\beta$ . These hydrophobic residues pack this helical segment to the framework. By contrast, in IL-1 $\beta$  the introduction of a tyrosine at the position equivalent to Leu87 and also Ser45 at the position equivalent to Val44, disrupts the hydrophobic patch. This loop in IL-1 $\beta$  contains the positively charged residues Lys93 and Lys94, which contact domain 3 of IL-1RI. In IL-1F5, the corresponding residues Tyr88, Glu93, and Lys95, whose side-chains are solvent exposed, would be accessible to interact with domain 3 of the cognate receptor, but presumably with a specificity distinct to that of IL-1 $\beta$ .

(v) Loop 11–12 of IL-1F5 has a four-residue insertion in it that extends this loop further out into the solvent perpendicular to the barrel axis. This loop may have functional implications for the molecule (see below).

**Structural Differences with IL-1Ra Suggest that IL-1F5 Is an Agonist.** IL-1Ra can bind to IL-1RI with high affinity by interacting with receptor domains 1 and 2. Antagonist properties are thought to be conferred by two features which prevent first binding to domain 3 of the receptor and second recruitment into the complex of the accessory protein. IL-

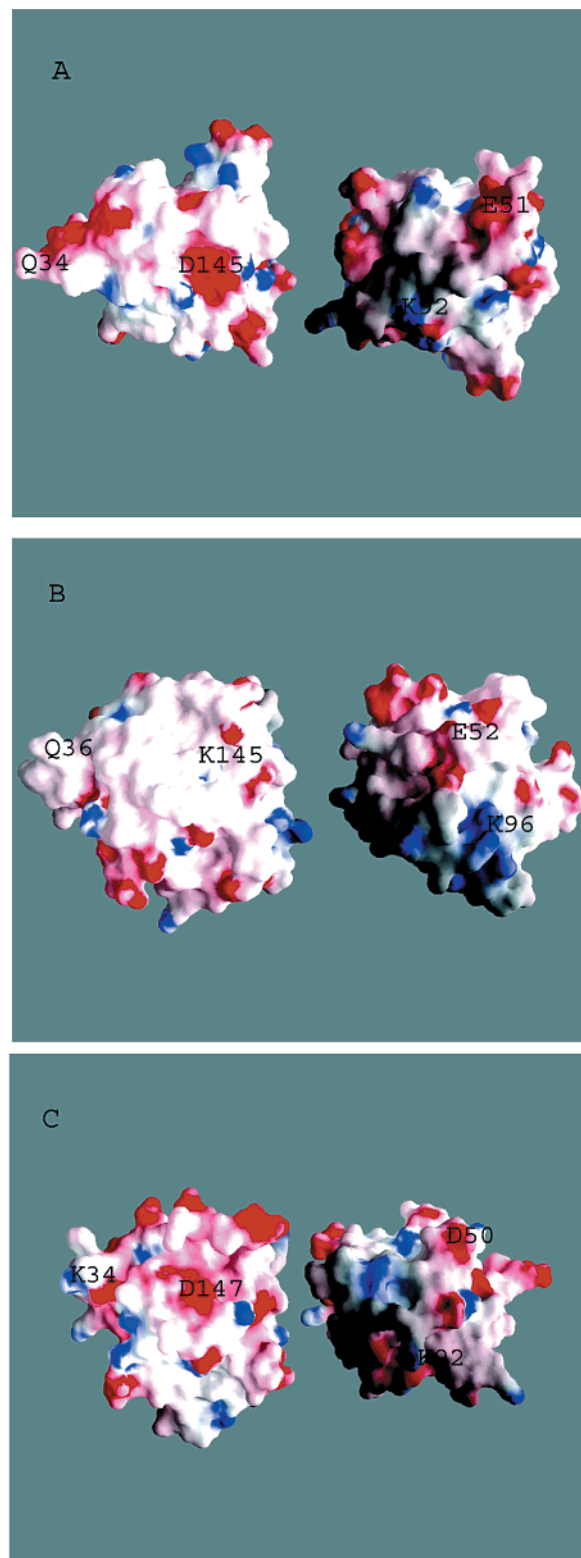


FIGURE 4: Electrostatic potential surface maps of (A) IL-1 $\beta$ , (B) IL-1Ra, (C) IL-1F5. Negative potential is red and positive potential is blue. Greatest saturation is at  $-10$  and  $+10$  kT. Molecules are viewed perpendicular to the barrel axis with face exposed from ligand/receptor complex shown (left) and from face that interacts with domain three of receptor (right). Diagrams were generated using GRASP.

1Ra has a deletion of six residues (49–55) in loop 4–5 as compared with both IL-1 $\beta$  and IL-1F5 (see Figures 1 and 3b,c). When loop 4–5 from IL-1 $\beta$  is inserted into IL-1Ra, it confers partial agonist properties (26). The composition

of this loop in IL-1F5 is different from that of IL-1 $\beta$ , and two residues that make important polar contacts with the receptor domain 3 (Gln48 and Asn53) are replaced by Arg and Ala, respectively, in IL-1F5, a finding that again argues for a different receptor specificity. The second difference concerns residue 147 which is an aspartic acid in both IL-1 $\beta$  and IL-1F5 but lysine in IL-1Ra. This residue is not involved in binding to the receptor but if the lysine is changed to aspartic acid, IL-1Ra gains partial agonist character (14, 26). In this case, it is thought that recruitment of accessory protein, a necessary event for signaling, requires this aspartate residue. Consistent with this idea, the electrostatic surface of IL-1F5 is more similar to that of IL-1 $\beta$  in this region (Figure 4). The region around residue 147 in IL-1Ra has a relatively featureless electrostatic surface, but by contrast IL-1 $\beta$  has a large negative potential due to the presence of Asp145, surrounded by smaller positive patches contributed by Lys138 and Lys109. This is conserved on the surface of IL-1F5 by the presence of Asp147 and Arg104.

**Modeling and Docking Studies Indicate that IL-1F5 Does Not Bind IL-1R but May Be a Ligand for an Orphan IL-1R Family Receptor.** We have used both superimposition and docking methods to assess whether IL-1F5 might bind to IL-1R. Both these approaches reveal numerous clashes between side-chains in the loops and the corresponding binding sites in the receptor. For example, loops 3–4, 4–5, and 7–8, all of which are involved in binding in IL-1 $\beta$ , and also loop 10–11 and 11–12, make clashes with domain 2 of the receptor (see Table SII, Supporting Information for details). In support of this conclusion, we find that IL-1F5 does not cause IL-1 responses such as activation of NF $\kappa$ B when applied to IL-1 responsive cell lines nor does it block IL-1 or IL-18 signaling (data not shown) (6). It is possible therefore that IL-1F5 binds one of the orphan IL-1 receptor family members and the most likely candidate is IL-1Rrp2. Recently, it has been shown that IL-1F5 can block the effects of IL-1F9 in Jurkat cells transfected with IL-1Rrp2, although no direct binding assays were performed (7). Although the study on IL-1Rrp2 implied that IL-1F5 might act as an antagonist, curiously no antagonism of the binding of IL-1F9 by IL-1F5 was reported. It is therefore possible that IL-1F5 might induce a signal that would block the function of this receptor indirectly. Attempts to dock IL-1F5 with a modeled structure of IL-1Rrp2 proved inconclusive possibly because interdomain flexibility is likely to cause large inaccuracies in the model.

In conclusion, despite the high sequence identity to IL-1Ra, which is largely due to the  $\beta$ -strand framework and not the loops, our structure predicts that IL-1F5 is an agonist for an orphan receptor containing three Ig domains. Our work suggests that distinct receptor specificities in the IL-1 cytokine family are caused by the evolution of distinct loop conformations and that the short helical segments joining loops 3 to 4 and 7 to 8 may be of particular importance.

## ACKNOWLEDGMENT

We thank the staff in Protein and Nucleic Acid Chemistry facility in Department of Biochemistry, University of Cambridge for help with mass spectrometric analysis and N-terminal sequencing, the staff of beamline ID14.2 and 14.7, ESRF, France, for help in data collection, and Nicholas

Harmer and Prof. Sir Tom Blundell for reading the manuscript and helpful comments. Science Foundation Ireland is acknowledged for funding to L.A.N.

## SUPPORTING INFORMATION AVAILABLE

Details of phase determination and structure refinement of single IL-1F5 crystal. Tables of crystal contact analysis for the IL-1 and receptor complex. This material is available free of charge via the Internet at <http://pubs.acs.org>.

## REFERENCES

- O'Neill, L. A., and Dinarello, C. A. (2000) The IL-1 receptor/toll-like receptor superfamily: crucial receptors for inflammation and host defense. *Immunol. Today* 21, 206–9.
- Sims, J. E. (2002) IL-1 and IL-18 receptors, and their extended family. *Curr. Opin. Immunol.* 14, 117–22.
- O'Neill, L. A. J., and Greene, C. (1998) Signal transduction pathways activated by the IL-1 receptor family: ancient signaling machinery in mammals, insects, and plants. *J. Leukocyte Biol.* 63, 650–657.
- Eisenberg, S. P., Evans, R. J., Arend, W. P., Verderber, E., Brewer, M. T., Hannum, C. H., and Thompson, R. C. (1990) Primary structure and functional expression from complementary DNA of a human interleukin-1 receptor antagonist. *Nature* 343, 341–6.
- Dunn, E., Sims, J. E., Nicklin, M. J., and O'Neill, L. A. (2001) Annotating genes with potential roles in the immune system: six new members of the IL-1 family. *Trends Immunol.* 22, 533–6.
- Barton, J. L., Herbst, R., Bosisio, D., Higgins, L., and Nicklin, M. J. (2000) A tissue specific IL-1 receptor antagonist homolog from the IL-1 cluster lacks IL-1, IL-1ra, IL-18, and IL-18 antagonist activities. *Eur. J. Immunol.* 30, 3299–308.
- Debets, R., Timans, J. C., Homey, B., Zurawski, S., Sana, T. R., Lo, S., Wagner, J., Edwards, G., Clifford, T., Menon, S., Bazan, J. F., and Kastelein, R. A. (2001) Two novel IL-1 family members, IL-1 delta and IL-1 epsilon, function as an antagonist and agonist of NF-kappa B activation through the orphan IL-1 receptor-related protein 2. *J. Immunol.* 167, 1440–6.
- Finkel, B. C., Clancy, L. L., Holland, D. R., Muchmore, S. W., Watenpugh, K. D., and Einspahr, H. M. (1989) Crystal structure of recombinant human interleukin-1 beta at 2.0 Å resolution. *J. Mol. Biol.* 209, 779–91.
- Clore, G. M., Driscoll, P. C., Wingfield, P. T., and Gronenborn, A. M. (1990) Analysis of the backbone dynamics of interleukin-1 beta using two-dimensional inverse detected heteronuclear <sup>15</sup>N-<sup>1</sup>H NMR spectroscopy. *Biochemistry* 29, 7387–401.
- Vigers, G. P., Caffes, P., Evans, R. J., Thompson, R. C., Eisenberg, S. P., and Brandhuber, B. J. (1994) X-ray structure of interleukin-1 receptor antagonist at 2.0-Å resolution. *J. Biol. Chem.* 269, 12874–9.
- Schreuder, H. A., Rondeau, J. M., Tardif, C., Soffientini, A., Sarubbi, E., Akesson, A., Bowlin, T. L., Yanofsky, S., and Barrett, R. W. (1995) Refined crystal structure of the interleukin-1 receptor antagonist. Presence of a disulfide link and a cis-proline. *Eur. J. Biochem.* 227, 838–47.
- Vigers, G. P., Anderson, L. J., Caffes, P., and Brandhuber, B. J. (1997) Crystal structure of the type-I interleukin-1 receptor complexed with interleukin-1beta. *Nature* 386, 190–4.
- Schreuder, H., Tardif, C., Trump-Kallmeyer, S., Soffientini, A., Sarubbi, E., Akesson, A., Bowlin, T., Yanofsky, S., and Barrett, R. W. (1997) A new cytokine-receptor binding mode revealed by the crystal structure of the IL-1 receptor with an antagonist. *Nature* 386, 194–200.
- Ju, G., Labriola-Tompkins, E., Campen, C. A., Benjamin, W. R., Karas, J., Plocinski, J., Biondi, D., Kaffka, K. L., Kilian, P. L., Eisenberg, S. P., and et al. (1991) Conversion of the interleukin 1 receptor antagonist into an agonist by site-specific mutagenesis. *Proc. Natl. Acad. Sci. U.S.A.* 88, 2658–62.
- Leslie, A. G. W., Brick, P., and Wonacott, A. T. (1986) TMOSFLM, *Daresbury Lab Inf. Quart. Protein Crystallogr.*, 18, 33–39.
- Potterton, E., McNicholas, S., Krissinel, E., Cowtan, K., and Noble, M. (2002) The CCP4 molecular-graphics project. *Acta Crystallogr. D Biol. Crystallogr.* 58, 1955–7.
- Thompson, J. D., Higgins, D. G., and Gibson, T. J. (1994) CLUSTAL W: improving the sensitivity of progressive multiple

- sequence alignment through sequence weighting, position-specific gap penalties and weight matrix choice. *Nucleic Acids Res.* 22, 4673–80.
18. Sali, A., and Blundell, T. L. (1993) Comparative protein modelling by satisfaction of spatial restraints. *J. Mol. Biol.* 234, 779–815.
  19. Laskowski, R. A., Moss, D. S., and Thornton, J. M. (1993) Main-chain bond lengths and bond angles in protein structures. *J. Mol. Biol.* 231, 1049–67.
  20. Katchalski-Katzir, E., Shariv, I., Eisenstein, M., Friesem, A. A., Aflalo, C., and Vakser, I. A. (1992) Molecular surface recognition: determination of geometric fit between proteins and their ligands by correlation techniques. *Proc. Natl. Acad. Sci. U.S.A.* 89, 2195–9.
  21. Eriksson, A. E., Cousens, L. S., Weaver, L. H., and Matthews, B. W. (1991) Three-dimensional structure of human basic fibroblast growth factor. *Proc. Natl. Acad. Sci. U.S.A.* 88, 3441–5.
  22. Habazettl, J., Gondol, D., Wiltsccheck, R., Otlewski, J., Schleicher, M., and Holak, T. A. (1992) Structure of hisactophilin is similar to interleukin-1 beta and fibroblast growth factor. *Nature* 359, 855–8.
  23. Sweet, R. M., Wright, H. T., Janin, J., Chothia, C. H., and Blow, D. M. (1974) Crystal structure of the complex of porcine trypsin with soybean trypsin inhibitor (Kunitz) at 2.6-Å resolution. *Biochemistry* 13, 4212–28.
  24. Murzin, A. G., Lesk, A. M., and Chothia, C. (1992) beta-Trefoil fold. Patterns of structure and sequence in the Kunitz inhibitors interleukins-1 beta and 1 alpha and fibroblast growth factors. *J. Mol. Biol.* 223, 531–43.
  25. Sibanda, B. L., Blundell, T. L., and Thornton, J. M. (1989) Conformation of beta-hairpins in protein structures. A systematic classification with applications to modelling by homology, electron density fitting and protein engineering. *J. Mol. Biol.* 206, 759–77.
  26. Greenfeder, S. A., Varnell, T., Powers, G., Lombard-Gillooly, K., Shuster, D., McIntyre, K. W., Ryan, D. E., Levin, W., Madison, V., and Ju, G. (1995) Insertion of a structural domain of interleukin (IL)-1 beta confers agonist activity to the IL-1 receptor antagonist. Implications for IL-1 bioactivity. *J. Biol. Chem.* 270, 22460–6.
  27. Shi, J. Y., Blundell, T. L., and Mizuguchi, K. (2001) FUGUE: Sequence-structure homology recognition using environment-specific substitution tables and structure-dependent gap penalties. *J. Mol. Biol.* 310, 243–257.
  28. Esnouf, R. M. (1997) An extensively modified version of MolScript that includes greatly enhanced coloring capabilities, *J. Mol. Graph. Model.* 15, 132–4, 112–3.
  29. Kabsch, W., and Sander, C. (1983) Dictionary of protein secondary structure: pattern recognition of hydrogen-bonded and geometrical features. *Biopolymers* 22, 2577–637.

BI0341197